Aerosol and Air Quality Research

ORIGINAL RESEARCH
https://doi.org/10.4209/aaqr.200625

Impact of Wheat Harvest on Levels and Sources of $PM_{2.5}$-associated PAHs in an Urban Area Located at the Center of Beijing-Tianjin-Hebei Region

Zhiyong Li[1,2*], Zhenxin Li[1], Ziyuan Yue[1], Dingyuan Yang[1], Yutong Wang[1], Lan Chen[1,2], Songtao Guo[1], Jinsong Yao[1], Lei Wang[3], Xiao Lou[1], Xiaolin Xu[1], Jinye Wei[1], Baole Deng[4*], Hong Wu[5]

[1] A Hebei Key Lab of Power Plant Flue Gas Multi-Pollutants Control, Department of Environmental Science and Engineering, North China Electric Power University, Baoding 071003, China
[2] MOE Key Laboratory of Resources and Environmental Systems Optimization, Ministry of Education, Beijing 102206, China
[3] Hebei Research Center for Geoanalysis, Baoding 071003, China
[4] Tianjin Eco-Environmental Monitoring Center, Tianjin 300191, China
[5] College of Environment and Resources, Chongqing Technology and Business University, Chongqing 400067, China

ABSTRACT

Wheat harvest and subsequent straw burning for maize planting can cause severe $PM_{2.5}$ and PAH pollutions and deteriorate the air quality of nearby cities in consequence. $PM_{2.5}$ samples were collected in Baoding urban area (BUA) from June 18 to July 7 of 2019, during and after wheat harvest (DWH and AWH, respectively). The "Migration Effect" (i.e., $PM_{2.5}$ and PAHs transferred from rural to urban during DWH and AWH, respectively) was proved by both the later time for appearance of peak values of $PM_{2.5}$ and PAHs and the air mass origins in BUA. The daily average $PM_{2.5}$ (reported in μg m^{-3}) 137 of DWH was 2.58 times 53.1 of AWH for BUA, regardless of its lower levels than the corresponding 156 and 75.6 for an adjacent rural site (ARS). The reverse trend was found for PAH mass contents (in μg g^{-1}), AWH possessed much higher value of 139 than 27.8 of DWH, while no significant fluctuations occurred for PAH concentrations due to the varied $PM_{2.5}$ levels. Four PAH sources including biomass burning (BB), coal combustion (CC), vehicle exhaust (VE) and industrial emissions (IN) were identified using positive matrix factorization (PMF). BB was the biggest contributor during whole sampling period (WSP), followed by CC, VE, and IN. BB increased from 17.3% to 37.1% along with the transition from DWH to AWH, indicated the impact of straw burning for maize planting. High share of CC suggested that coal was still an important civil fuel. The strict emission reduction measures made the industry smallest contributor in BUA. Lower VE share in BUA than ARS demonstrated that influence of high-intensity operation of wheat harvesters and rotary cultivators.

Keywords: $PM_{2.5}$, PAHs, PMF, Backward trajectory clustering, Wheat harvest

OPEN ACCESS

Received: November 10, 2020
Revised: December 27, 2020
Accepted: December 27, 2020

* **Corresponding Authors:**
Zhiyong Li
lzy6566@126.com
Baole Deng
dengbaolekobe@126.com

Publisher:
Taiwan Association for Aerosol Research
ISSN: 1680-8584 print
ISSN: 2071-1409 online

1 INTRODUCTION

Environmental contamination has also occurred along with the process of industrialization and urbanization in the past few decades in China. In recent years, more attention has been paid to the issues with frequent occurrence of haze and photochemical smog characterized by high loadings of particulate matter and ozone (Elorduy *et al.*, 2016; Cao *et al.*, 2018; Li *et al.*, 2020a, b). Fine particulate matter (especially $PM_{2.5}$) has received widespread attention due to its negative impact on air quality and human health (Li *et al.*, 2019a, 2019b). As a carrier for various toxic

organic compounds, $PM_{2.5}$ can be inhaled and absorbed into the human alveolar tissue and then cause damage to respiratory and cardiovascular systems, whose harm is more serious because of its smaller size (Li and Zhang, 2014; Lelieveld *et al*., 2015; Xiong *et al*., 2015; Zhang *et al*., 2019).

As a class of persistent organic pollutants (POPs), polycyclic aromatic hydrocarbons (PAHs) are widely found in the environmental mediums and always origin from incomplete incineration of coal, crop straws, garbage and the other organic substances (Xing *et al*., 2016; Han *et al*., 2019; Li *et al*., 2020b). They are extensively recognized as severe pollutants due to their carcinogenic and mutagenic properties with $PM_{2.5}$-bound PAHs accounting for more than 80% of particle associated PAHs (Dat *et al*., 2018; Simayi *et al*., 2018). Human lung cancer, which has become the fourth leading cause of death in China, is closely relevant to inhaled PAHs (Zhou *et al.,* 2016). Exposure to PAHs can give rise to impaired lung function, and asthma and thrombosis in patients with coronary heart disease (Zhou *et al*., 2016). Also PAHs possess negative impacts on the reproductive system and immune system due to their reactions with the hormone system (Garcia-Suastegui *et al*., 2011). The U.S. Environmental Protection Agency and the European Union had designated 16 PAH compounds as priority pollutants considering their potential health threats to people (Li *et al*., 2020b).

China possessed the highest PAHs emissions in the world, accounting for about 21% of global emissions by 2007 and the total emissions reached as high as 120,611 tons in 2012 (Shen *et al*., 2013; Li *et al*., 2019; Zhang *et al*., 2019b). Atmospheric PAHs in China are mainly derived from anthropogenic emissions including biomass burning, domestic coal combustion, coke production, traffic emissions and so on (Zhang and Tao, 2009; Cao *et al*., 2018). Previous studies also reported that biomass burning, domestic coal combustion, and coke production contributed 59%, 23%, and 15% to the total PAHs, respectively in China (Zhang *et al*., 2019a). As the strictest air pollution control policy in China, the Air Pollution Prevention and Control Action Plan (APPCAP; 2013–2017) was implemented to reduce the 25% $PM_{2.5}$ in main metropolitan areas by 2017 and markedly improve air quality (Zhai *et al*., 2019; Li *et al*., 2020b). $PM_{2.5}$ levels accordingly decreased by 30–50% on a national scale although there was still the certain gap with the threshold value designated by China Air Quality Standard Grade I. “Three Years Action Plan to Win the Blue Sky Defense War” (TYAP) putting forward “Clean Heating” in north China was launched in 2017 (Li *et al*., 2020b). “Coal Removal Campaign”, “Prohibition of Biomass Burning”, “Traffic Limitation”, “Ultra Low Emission Standard for Industrial Enterprises” and so on had rooted in APPCAP and TYAP (Zhai *et al*., 2019).

Although biomass burning had been banned since 2013, as the largest agricultural country, China still retains tradition of straw burning to prepare for the next crop cycle planting due to the requirement of fewer resources, elimination of undesirable weeds and pests and provision of nutrients to the soil. A large amount of particulate matter (PM), carbon monoxide (CO), volatile organic compounds (VOC) and a certain range of semi-volatile organic compounds (SVOCs) with PAHs included released from incomplete biomass combustion (Hays *et al*., 2005; Koss *et al*., 2018; Ravindra *et al*., 2019). In eastern China, wheat straw combustion contributes more than 50% to atmospheric particles (Li *et al*., 2014).

As the largest economic zones in the north of China, the Beijing-Tianjin-Hebei (BTH) region has been plagued by frequent air pollution incidents ascribed to the rapid economic development and the fast pace of urbanization, which had been the most heavily polluted region in China's urban agglomeration (Zhai *et al*., 2019). Biomass burning (BB) is the main source of $PM_{2.5}$ and PAHs in BTH (Zhang *et al*., 2017; Wang *et al*.,2018). BTH is an important wheat producing area and the annual wheat rotation season is from the end of June to the middle of July. The emissions from rural sites had been the important atmospheric pollutant sources to BTH urban areas (Li *et al*., 2020b). The evaluation of impact of wheat harvest and subsequent straw burning for next maize planting on PAHs of urban area is important to the improvement of urban air quality.

Baoding City with the worst air quality in BTH and located in the central area of BTH region. Our previous study has reported the PAHs characteristics for a central rural site of BTH related to wheat harvest period (Li *et al*., 2020b). This study analyzed the levels, sources and fluctuation trends of 18 $PM_{2.5}$-bound PAH congeners of Baoding to evaluate the impact of wheat harvest in rural area. The same $PM_{2.5}$ sampling campaign was adopted with our previous study for ARS in Wangdu County, 50 kilometers south of Baoding (Li *et al*., 2020b). The analysis of $PM_{2.5}$ and PAHs changes in BUA during DWH and AWH could facilitate a more comprehensive assessment of the

impact of wheat harvest activities on urban PAHs. The main purposes of this study were to: 1) analyze the changes of $PM_{2.5}$ and PAHs in BUA associated with wheat harvest and subsequent straw burning activities; 2) to analyze the origins of air masses using backward trajectory clustering; and 3) identify the sources of PAHs using Positive Matrix Factor (PMF) model.

2 METHDOLOGY

2.1 Sampling Area Description

As shown in Fig. 1, BUA locates in the northern part of the North China Plain (NCP) and central area of BTH region, which is 140 kilometers north of Beijing, 145 kilometers east of Tianjin and 125 kilometers southwest of Shijiazhuang. The sampling site is on the rooftop of a six-story Teaching Building (approximately 30 m above ground) in North China Electric Power University without tall buildings and industrial enterprises around. The other sampling site in our previous work, ARS was also shown in Fig. 1

2.2 $PM_{2.5}$ Sampling

$PM_{2.5}$ samples were consecutively collected by the medium-volume air samplers (TH-150C III, Wuhan Tianhong Ltd., China) at a flow of 100 L min^{-1} and a total of 40 samples were obtained. The 23 h integrated samples were gathered during June 18 to July 7, 2019 and each was conducted from 9:00 a.m. to 8:00 a.m. of the next day. Two air samplers were used to collect daily samples. One sampler was equipped with a quartz filter (QF, 1 μm pore size and 90 mm diameter, Pall USA Inc.) was used to analyze PAHs, and the another sampler installed with a Teflon filter (TEF, 1 μm pore size and 90 mm diameter, Whatman Co. UK) was used to obtain the $PM_{2.5}$ mass by subtracting pre-weight from post-weight. A set of field blank samples were simultaneously gathered by exposing filters in the sampler without airflow in drawing, to evaluate the subsequent analysis bias and precision. Prior to sampling, QFs were heated at 450°C for 4 h and TEFs were also heated at 60°C. TEFs were stored in a room with a constant 20°C and 50% of relative humidity before and after sampling for weighting (SartoriusME-5F, readability: 1 μg).

Meteorological parameters including the temperature, wind speed and direction were

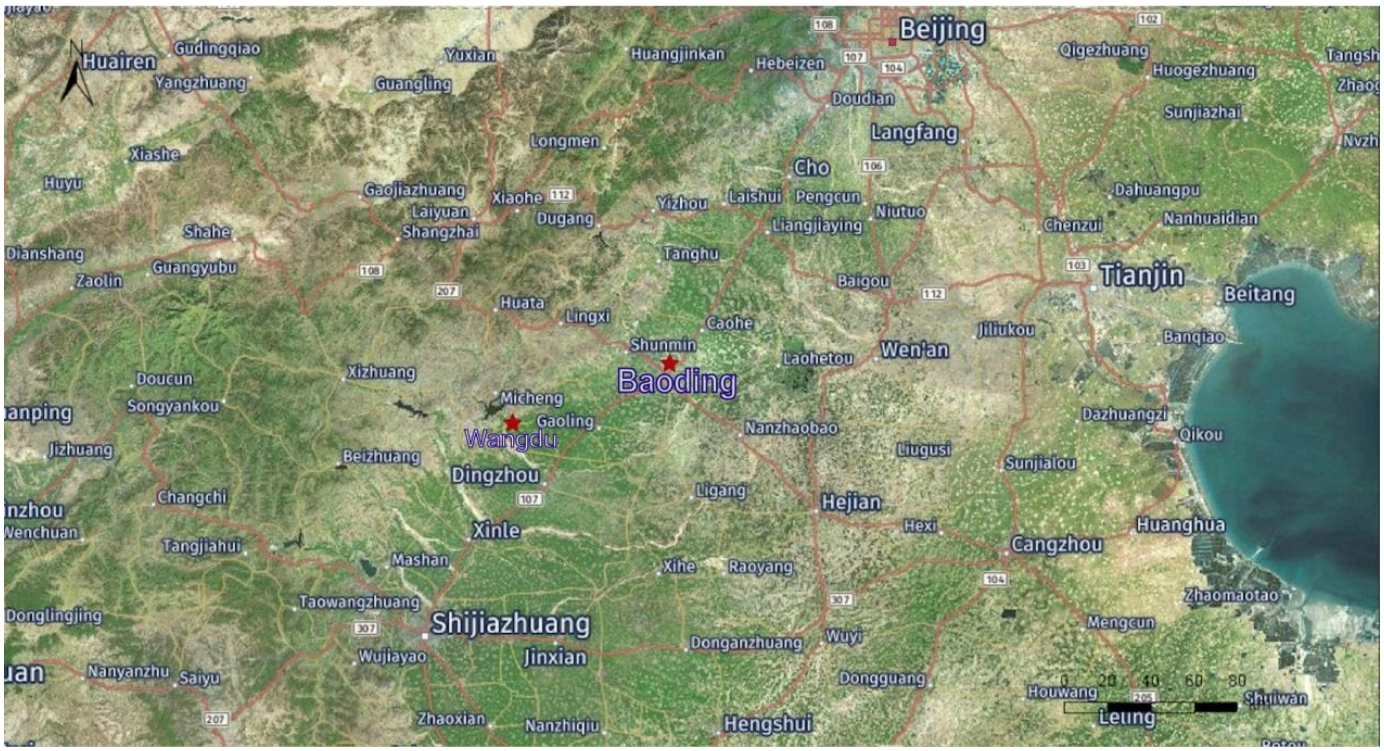

Fig. 1. Sampling location in North China Plain.

simultaneously recorded. The sensitivity of the weighing scale was set to ± 0.010 mg. The $PM_{2.5}$ concentrations were finally calculated as the quotient between $PM_{2.5}$ mass and corrected sampling air volume.

2.3 PAH Analysis Procedure

PAHs in QFs were analyzed using a gas chromatography/mass spectrometry system (HP6890 GC/MS 5973i). The same chromatographic conditions as TO-13 method were adopted in this study and shown as follows: 70°C held for 2 min, ramped to 260°C at 10°C min^{-1} and held for 8 min, then ramped to 300°C at 5°C min^{-1} and held for 5 min. Helium was used as the carrier gas at a constant flow of 1.0 mL min^{-1}. Detailed analysis procedures of GC-MS could be found in our previous work of Li *et al.* (2018, 2020b) and was described simply as follows: QF was extracted with an ultrasonic wave using dichloromethane and concentrated with a rotary evaporator. The extract was then purified in a gel column and concentrated again with a rotary evaporator. Finally, the volume was set at 0.5 mL by nitrogen blowing before analysis.

The 18 PAH congeners including naphthalene (NA), acenaphthylene (ACL), acenaphthene (AC), fluorine (Fl), benzo(g,h,i)peryene (BgP), phenanthrene(PHE), anthracene (AN), fluoranthene (FA), pyrene (PY), benzo(a)anthracene (BaA), chrysene (CHR), benzo(b)fluoranthene (BbF), benzo(k)fluoranthene (BkF), benzo(e)pyrene (BeP), benzo(a)pyrene (BaP), indeno(1,2,3-cd)pyrene (IP), dibenzo(a,h)anthracene (DBA) and coronene (COR) were involved in this study. The 18 PAHs were classified into different homologs based on their ring numbers and they were 2-ring (NA), 3-ring (ACL, AC, Fl, PHE, and AN), 4-ring (FA, PY, BaA, and CHR), 5-ring (BbF, BkF, BaP, and BeP), 6-ring (IP, DBA, and BgP) and 7-ring (COR). They were further divided to low molecular weight (LMW) (2- and 3-ring), middle molecular weight (MMW, 4-ring) and high molecular weight (HMW, 5-, 6-, and 7-ring) (Li *et al.*, 2018; Li *et al.*, 2020b).

The m/z values used to the PAH congener identification were 129, 127 for NA, 153, 152 for ACL, 151, 153 for AC, 165, 167 for Fl, 179, 176 for PHE and AN, 101, 203 for FA and PY, 229, 226 for BaA, 226, 229 for CHR, 256, 126 for BbF and BkF, 253, 126 for BaP and BeP, 138, 227 for IP, 139, 279 for DBA, 138, 227 for BgP, and 150, 301 for COR, respectively. Correspondingly, the quantitative m/z values were 128, 154, 152, 166, 178, 178, 202, 202, 228, 228, 252, 252, 252, 252, 276, 278, 276, 300 for NA, ACL, AC, FL, PHE, AN, FA, PY, BaA, CHR, BbF, BkF, BaP, BeP, IP, DBA, BgP and COR, respectively.

The entire pre-treatment and analysis procedures comply with the quality control/quality assurance (QC/QA) programs were strictly done. A series of experiments including sample blank, sample duplication, matrix spiked sample, and procedural blank were conducted on schedule every 5 samples to evaluate the accuracy of the analysis. No target chemicals were found in the solvent or procedural blank experiments. The method detection limits (MDLs) (reported in ng g^{-1}) of the 18 PAHs were in the 0.12–1, with a mean value of 0.230 ± 0.202. The recovery efficiency for the 18 PAHs in matrix added samples ranged from 80% to 121%. The surrogate standards including 14-deuterium substituted terphenyl and 4-bromo-2-fluorobiphenyl in 20 samples, possessed the recoveries of 90 ± 15% and 95 ± 20%, respectively. The variations of PAH detected concentrations in 4 duplicated samples were all less than 10%.

A total of 11 PAHs including BgP, IP, BbP, PHE, FA, BaA, CHR, PY, BaP, BeP and BkF were detectable in this study. Therefore, the sum of 11 PAHs (Σ_{11}PAHs) was used to represent the total PAHs.

2.4 Source Identification by PMF Model

The positive matrix factorization (PMF), a multivariate factor analysis tool, has advantages over PCA and CMB lies in elimination of negative factor loadings and no need of source profiles, is widely used for $PM_{2.5}$ source appointment (Bari and Kindzierski, 2016; Chen *et al.*, 2016; Yao *et al.*, 2016; Tan *et al.*, 2017). It can acquire more realistic source information based on the non-negative constraints. The EPA PMF (version5.0) was employed to identify and apportion the potential source contributions of $PM_{2.5}$-bound PAHs in this study. The model input datasets were consisted of PAH concentrations and corresponding uncertainties. The abnormal values were excluded to prevent error of PMF results.

The half of MDL was used to represent the PAH concentration below than MDL. The geometric mean of the observed values was used as substitute for missing values and associated uncertainties

were set as four times the geometric mean (Yao *et al*., 2016). Uncertainty, a key input, included detection limits and error fraction. Uncertainty data could be obtained by following equations:

For $c_i \leq$ MDL, unc = 5/6 × MDL (1)

For $c_i \geq$ MDL, unc = $[(c_i/5)^2+MDL^2]^{0.5}$ (2)

A total of 20 runs were used for each chemical component. The lowest Q_{robust} value was 3069.30, and the ratio of Q_{robust}/Q_{true} was 0.90.

2.5 Backward Trajectory Clustering Analysis

Backward trajectory clustering analysis can identify the potential geographic origins of PAHs and is a key tool to simulate the trajectories of air pollutants. Three dimensional 72 h backward trajectories of air masses arriving at Baoding were calculated using the Hybrid Single Particle Lagrangian Integrated Trajectory (HYSPLIT-4) model. According to the properties and methods of the clustering trajectory map, the trajectories were divided into four paths and the uniformity of the trajectory was reflected at the minimum angle.

3 RESULT AND DISCUSSION

3.1 Levels of $PM_{2.5}$ and $PM_{2.5}$-bounded PAHs

The $PM_{2.5}$ and PAH concentrations as well as PAH contents for each sampling day, DWH and AWH in BUA were shown in Fig. 2. The $PM_{2.5}$ concentrations during DWH varied from 107 to 156 μg m^{-3} and averaged as 137 ± 26.1 μg m^{-3}, while those of AWH fluctuated from 1.96 to 155 μg m^{-3} and it was 53.1 ± 38.0 μg m^{-3} on average. The daily average $PM_{2.5}$ of DWH was more than twice that of AWH indicating the strong influence of large amounts of fugitive dust generated from the wheat harvest and transportation (Li *et al*., 2020b). The daily average $PM_{2.5}$ during DWH in BUA was 3–4 times the 35 μg m^{-3} of National Air Quality Standard Grade I and substantially

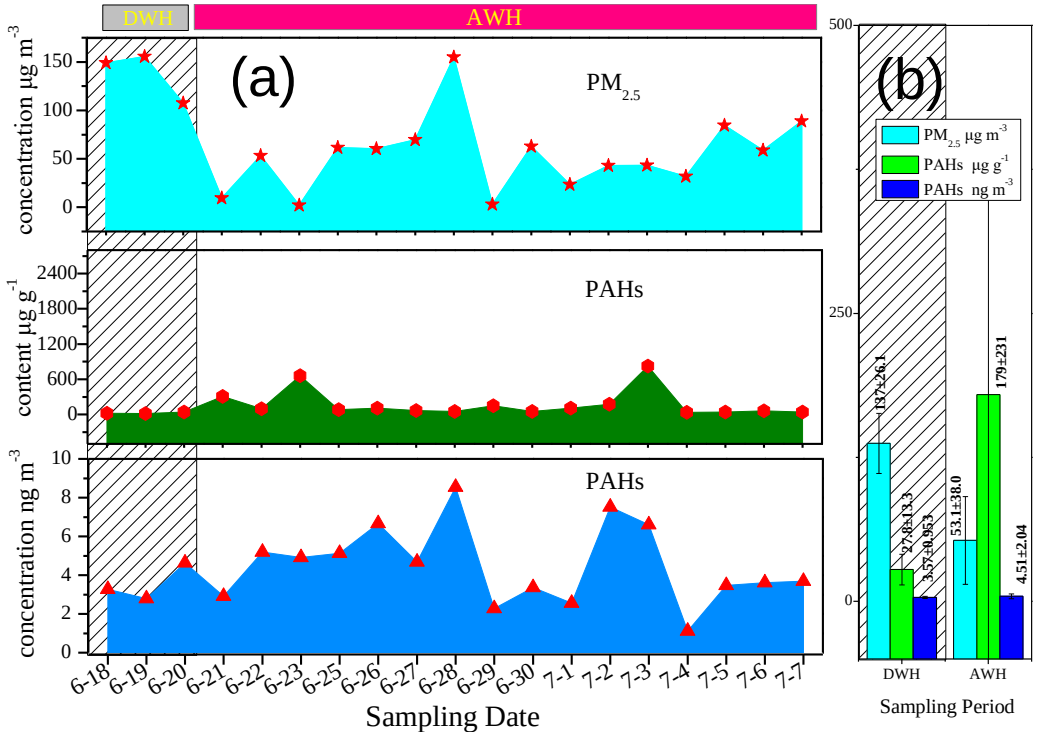

Fig. 2. $PM_{2.5}$ concentrations, PAH contents, and PAH concentrations for each sampling day (a), and (b) DWH and AWH period.

higher than the daily average $PM_{2.5}$ of 65 μg m^{-3} for cities in northern China, which indicated the adverse effect of wheat harvest on $PM_{2.5}$ levels (Ding *et al.*, 2019; Zhai *et al.*, 2019). BUA possessed much higher $PM_{2.5}$ concentrations than those five urban agglomerations in 2018, which were 55 μg m^{-3} for BTH, 62 μg m^{-3} for Fenwei Plain (Xi'an), 40 μg m^{-3} for Sichuan Basin, 40 μg m^{-3} for Yangtez River Delta, and 31 μg m^{-3} for Pearl River Delta, respectively (Zhai *et al.*, 2019). The corresponding $PM_{2.5}$ during AWH was much lower than 75 μg m^{-3} designated by National Air Quality Standard Grade II regardless of it was close to 2 times value of Grade I, which implied the positive effects of straw open burning prohibition in recent China. Higher $PM_{2.5}$ than Grade I during AWH also indicated the straw burning still existed in some rural areas. The air quality improvement by $PM_{2.5}$ decrease would be achieved by the completely ban of straw burning during post-harvest period (Cheng *et al.*, 2014).

The $PM_{2.5}$ concentrations showed a generally downward trend from June 18 to June 20 reflected the wheat harvest activities for surround rural areas of BUA entered the final stage. BUA showed the similar $PM_{2.5}$ fluctuation trends with ARS in Wangdu County during DWH in spite of the its relative low $PM_{2.5}$ levels, which implied the migration effects of regional particles (Li *et al.*, 2020b).

Triggered by the crisis of high $PM_{2.5}$, China launched the "Air Pollution Prevention and Control Action Plan" (APPCAP) during 2013–2017, the national emission of primary $PM_{2.5}$ reduced by 33% in consequence and $PM_{2.5}$ levels in Beijing-Tianjin-Hebei (BTH) region basically reached the National Air Quality Standard Grade II (Cheng *et al.*, 2019; Zhai *et al.*, 2019). However, $PM_{2.5}$ associated with wheat harvest in a central rural area of BTH and BUA incompatibly reached up to 156 μg m^{-3} and 137 μg m^{-3}, indicating it was necessary to develop effective measures to reduce $PM_{2.5}$ emissions from wheat harvest and subsequent open straw burning (Li *et al.*, 2020b). It should be noted that the elevated $PM_{2.5}$ levels during DWH were still lower than those before the implementation of APPCAP confirmed its effectiveness for $PM_{2.5}$ decline (Li *et al.*, 2020b). However, DWH possessed substantially higher $PM_{2.5}$ than those after APPCAP.

The $PM_{2.5}$ concentrations of ARS in Wangdu County during AWH peaked on June 25 (140 μg m^{-3}), June 26(110 μg m^{-3}) and June 28 (120 μg m^{-3}), while the corresponding peaks appeared on June 27 (69.5μg m^{-3}), June 28 (154 μg m^{-3}) and June 30 (62.7 μg m^{-3}) subsequently in BUA, implied the occurrence of pollutant diffusion model of "Rural Surrounding City". Trans-regional migration of the air pollutants derived from open burning of wheat straw after harvest would worsen the air quality of urban area (Li *et al.*, 2020b).

Much higher PAH mass contents were found during AWH compared with those during DWH implying the strong impact of PAH emissions from open wheat straw burning (Fig. 2). The PAH mass contents during DWH varied from 18.0 to 43.0 μg g^{-1} and averaged as 27.8 μg g^{-1}, while they fluctuated from 34.9 to 825 μg g^{-1} with a mean up to 179 μg g^{-1} during AWH. It should be noted that total PAH contents peaked on June 22 and July 2 in ARS and the highest PAHs of BUA accordingly appeared on subsequent June 23 and July 3 in consequence, which suggested the wheat straw burning associated PAHs migrated from ARS to BUA (Li *et al.*, 2020b). More than 40% of air masses originated from southern Baoding and trajectories arrived at BUA on June 23 and July 3 even reached up to 81.2%, which further verified the occurrence of the "Migration Effect" for PAHs. It should be concluded that straw burning after harvest characterized as low cost and easily operate still remained as an important practice in some rural areas regardless of the open straw burning prohibition in China. The mass volume concentrations of PAHs exhibited the different trends with PAH contents ascribed to the varied $PM_{2.5}$ concentrations. The PAH volume concentrations (reported in ng m^{-3}) for DWH were in the range of 2.80–4.64 and averaged as 3.57, and they varied from 1.11 to 8.55 with a mean value as 4.51 for AWH. The lower levels of $PM_{2.5}$ of AWH compared with DWH weaken the difference of PAH volume concentrations between them.

3.2 Contents and Concentrations of the Individual PAH Congener and Ring Size Distribution

The contents and concentrations of 11 individual PAHs (Σ_{11}PAHs) in each sampling day were shown in Fig. 3. Tables 1 and 2 listed the statistic values of PAH contents and concentrations for each PAH. All the 11 PAHs showed the same fluctuation trends during the sampling period for both contents and concentrations, while the vast differences existed between concentrations and

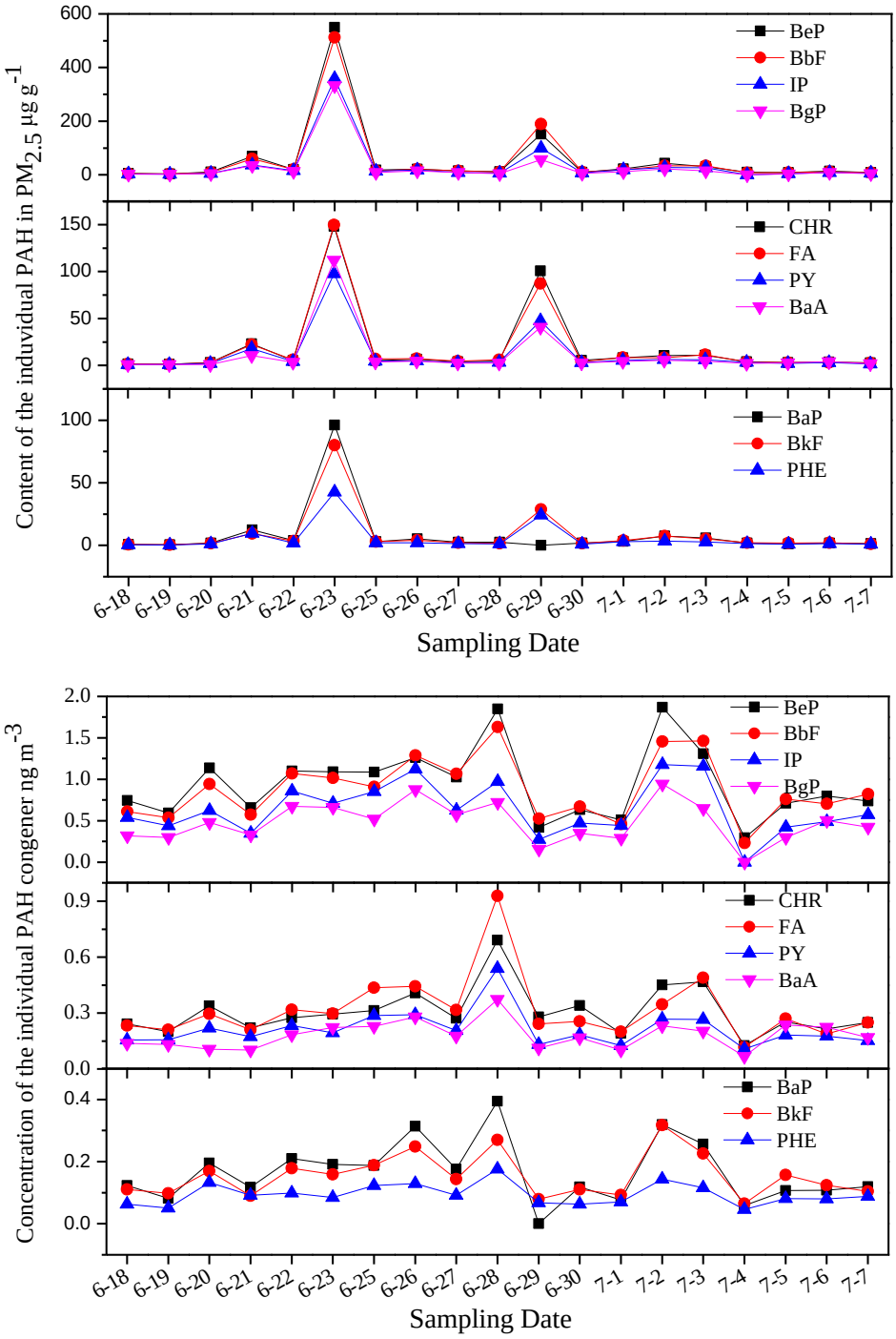

Fig. 3. Time series of the PAH contents and PAH concentrations for each PAH congener during whole sampling period.

contents for each PAH due to the varied $PM_{2.5}$ concentrations. The peak values for concentration and content occurred in different sampling date furtherly confirmed the impact of varied $PM_{2.5}$ levels. The total PAH mass contents peaked on June 23 and 29 for BUA, the corresponding values occurred on June 22 and July 3. The peak value of June 23 might be related to the PAH migration from ARS to BUA, while it might be associated with vehicle emissions for July 3. The highest contributions of biomass burning on June 23 and vehicle exhaust on July 3 would be the explanations (Figs. 3 and 6). For PAH mass concentrations, they peaked on June 26, 28, July 2 and 3 due to the varied $PM_{2.5}$ levels and contributions of different sources. The dispersed peaks of PAH contents suggested the contingency of straw burning during AWH.

Table 1. Mass content of each PAH in $PM_{2.5}$ (μg g^{-1}).

PAHs	DWH			AWH		
	Max	Min	Mean	Max	Min	Mean
BgP	4.42	1.91	2.84 ± 1.38	332	0	35.9 ± 83.3
IP	5.78	2.82	4.10 ± 1.52	359	0	43.5 ± 90.4
BkF	1.57	0.630	0.986 ± 0.508	80.1	1.74	10.4 ± 20.4
BbF	8.72	3.44	5.45 ± 2.86	512	7.23	64.6 ± 132
PHE	1.23	0.323	0.664 ± 0.496	42.5	0.959	6.58 ± 11.6
FA	2.73	1.35	1.90 ± 0.737	150	3.19	22.1 ± 41.1
BaA	0.982	0.841	0.923 ± 0.073	112	2.11	13.7 ± 28.9
CHR	3.14	1.29	2.03 ± 0.980	148	2.99	22.8 ± 42.5
PY	2.03	1.01	1.37 ± 0.574	97.6	2.16	14.2 ± 2.58
BaP	1.81	0.524	1.06 ± 0.669	96.2	0	9.95 ± 24.1
BeP	10.5	3.81	6.49 ± 3.56	549	8.38	66.1 ± 139
COR	n.d.	n.d.	n.d.	n.d.	n.d.	n.d.
DBA	n.d.	n.d.	n.d.	n.d.	n.d.	n.d.
NA	n.d.	n.d.	n.d.	n.d.	n.d.	n.d.
ACL	n.d.	n.d.	n.d.	n.d.	n.d.	n.d.
AC	n.d.	n.d.	n.d.	n.d.	n.d.	n.d.
FL	n.d.	n.d.	n.d.	n.d.	n.d.	n.d.
AN	n.d.	n.d.	n.d.	n.d.	n.d.	n.d.

Table 2. Volume concentrations of each PAH congener in air (ng m^{-3}).

PAHs	DWH			AWH		
	Max	Min	Mean	Max	Min	Mean
BgP	0.295	0.210	0.246 ± 0.043	0.928	0.116	0.332 ± 0.188
IP	0.133	0.050	0.082 ± 0.042	0.176	0.046	0.097 ± 0.033
BkF	1.14	0.595	0.825 ± 0.272	1.87	0.294	0.959 ± 0.459
BbF	0.195	0.082	0.133 ± 0.057	0.394	0.000	0.172 ± 0.106
PHE	0.941	0.536	0.695 ± 0.204	1.63	0.230	0.915 ± 0.399
FA	0.477	0.297	0.364 ± 0.091	0.942	0.000	0.497 ± 0.256
BaA	0.169	0.098	0.126 ± 0.036	0.318	0.065	0.160 ± 0.074
CHR	0.624	0.440	0.534 ± 0.092	1.18	0.000	0.656 ± 0.343
PY	0.137	0.106	0.125 ± 0.016	0.374	0.067	0.192 ± 0.076
BaP	0.339	0.200	0.260 ± 0.069	0.691	0.125	0.315 ± 0.136
BeP	0.219	0.155	0.177 ± 0.033	0.539	0.108	0.220 ± 0.103
COR	n.d.	n.d.	n.d.	n.d.	n.d.	n.d.
DBA	n.d.	n.d.	n.d.	n.d.	n.d.	n.d.
NA	n.d.	n.d.	n.d.	n.d.	n.d.	n.d.
ACL	n.d.	n.d.	n.d.	n.d.	n.d.	n.d.
AC	n.d.	n.d.	n.d.	n.d.	n.d.	n.d.
FL	n.d.	n.d.	n.d.	n.d.	n.d.	n.d.
AN	n.d.	n.d.	n.d.	n.d.	n.d.	n.d.

The Σ_{11}PAHs peaks for ARS occurred not only earlier than but also closed to those of BUA suggesting the impact of migration of straw burning associated PAHs from ARS to BUA. BeP was the predominant PAH considering PAH mass contents for both DWH (3.81–10.5 μg g^{-1} and averaged as 6.49) and AWH (8.25–549 μg g^{-1} and averaged as 62.5) (Table 1). In addition, BbF, IP, BgP, CHR and FA also dominated in both DWH and AWH considering their mass contents. In regard to PAH mass concentrations, the vast fluctuation occurred for each PAH congener indicated the different contributions of emission sources. BeP, BbF, IP, BgP, FA and CHR also dominated in DWH and AWH based on their mass contributions, accounting for 69%-84% of the total PAHs, and they were 0.825 ± 0.279, 0.695 ± 0.216, 0.534 ± 0.092, 0.364 ± 0.098 and 0.246 ± 0.044 ng m^{-3} for

DWH and 0.959 ± 0.459, 0.915 ± 0.399, 0.656 ± 0.343, 0.497 ± 0.256, 0.332 ± 0.188 and 0.315 ± 0.136 ng m^{-3} for AWH, respectively (Table 2).

The 5 top PAHs in ARS of Wangdu County were BeP, BbF, IP, BgP, and COR based on both mass contents and concentrations. The dominant PAH congeners between two places were roughly the same, indicating that the PAH pollution sources in two regions were roughly similar (Li *et al*., 2020b). Certain concentration of BaP was found for both DWH and AWH, which should be paid more attention due to its severe toxicity (Li *et al*., 2018).

Fig. 4 showed the ring size distribution patterns of PAHs during DWH and AWH for each sampling day. The 5-ring PAHs dominated in all the sampling days, followed by the 6- and 4-ring PAHs, while the 3-ring PAHs possessed the lower contributions. During whole sampling period, HMW-PAHs were predominant congeners. Along with the transition from DWH to AWH, the contribution ratios of 5- and 6-ring PAHs decreased from 49.3% to 48.9% and from 25.4% to 24.1%, while 4- and 3-ring PAHs increased from 23.1% to 24.6% and from 2.21% to 2.34%, respectively, which reflected the differences of source contributions between DWH and AWH. For ARS in Wangdu County, 5-ring PAHs increased from 42.3% to 46.7%, while the 6-ring PAHs decreased from 30.9% to 26.6%. The similar contribution ratios between ARS and BUA indicated that the surrounding straw burning phenomenon had a certain impact on the urban area. The 2-, 3-, and 4-ring PAHs dominated in particles emitted from the straw burning would be the explanation of enhanced levels of 4-ring PAHs (Li *et al*., 2018).

3.3 Source Apportionment of PAHs by PMF Model

PMF model was employed to apportion the potential pollution sources and four source profiles were obtained (Fig. S1). Factor 1 was characterized by high loadings of BbF, IP, FA, BeP and CHR, and medium to high loadings of PY and BaA. Also, high proportions of 4–5 ring PAHs were found in Factor 1 and it was assigned to represent vehicle exhaust (VE) (Zhou *et al*., 2005). The high number of private cars and the peak summer travel during summer vacation verified the VE exist. Factor 2 possessed high loadings of HMW-PAHs like IP and BgP and low levels were found for LMW- and MMW-PAHs including PHE, PY, FA and CHR, which was identified as coal combustion (CC) (Zhou *et al*., 2005; Li *et al*., 2020b). In consideration of Factor 3, the highest loading of BeP and BaP, and the low contents of LMW-PAHs such as FA, CHR and PY were found. Also the highest levels of 5-ring PAHs and certain amounts of PAHs with other ring numbers were found and Factor 3

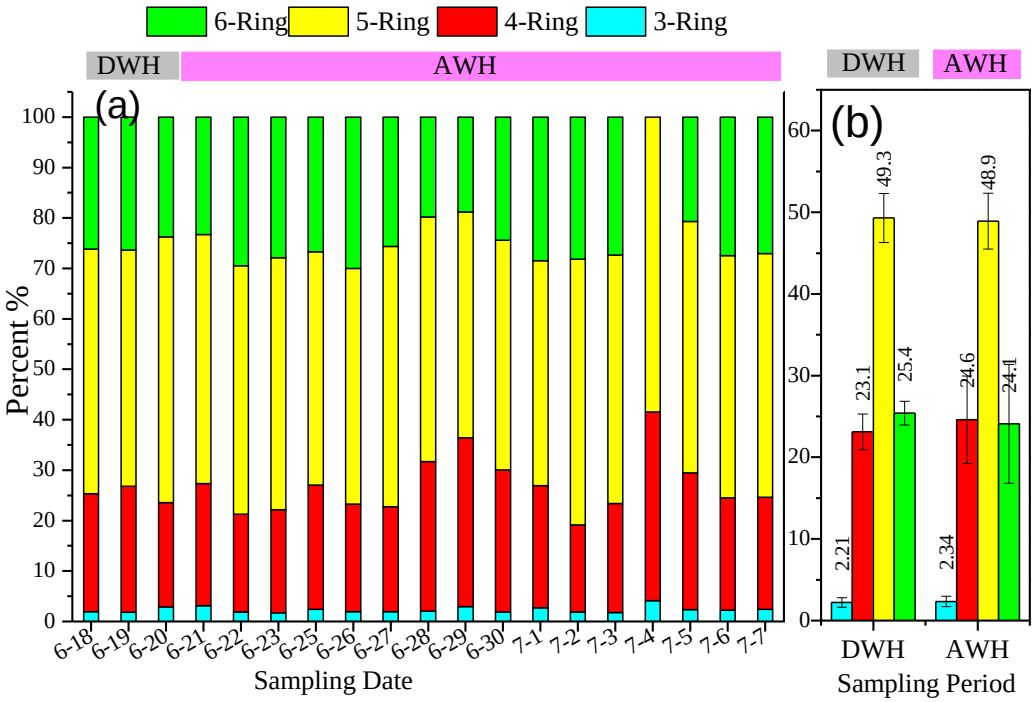

Fig. 4. PAH rings size distributions for (a) each sampling day, and (b) DWH and AWH periods.

was consequently recognized as biomass burning (BB) (Li *et al.*, 2020b). In regard to Factor 4, there was a high loading of 3- to 5-ring PAHs such as FA, CHR, and BbF, while low contents occurred for PAHs with higher ring number than 5 including IP and BgP. It was designed as industrial emissions (IN) accordingly There are a lot of factories in the east of BUA and adjacent rural areas, which may be the PAH emission source.

Fig. 5 showed the contributions of four sources including CC, VE, BB, and IN for DWH, AWH and WSP. For USA during WSP, BB possessed the highest contribution ratio of 34.4%, followed by 25.3% of CC, 22.5% of VE, and 17.8% of IN. The substantially different source contribution pattern was found in ARS, which was VE (30.8%) > BB (27.6%) > CC (27.5%) > IN (14.1%) (Li *et al.*, 2020).

The lowest IN contribution ratio was found for both BUA and ARS, which implied the effectiveness of recent emission control measures. The higher VE proportion surprisingly occurred in ARS instead of BUA suggested the strong impact of running of harvesters and rotary tillers with high intensity in ARS during WSP. The implausible appearance of highest BB contribution ratio in BUA was mainly ascribed to the decreasing shares of VE and CC. CC possessed slightly lower share in BUA than that of ARS, which indicated coal was still the important fuel regardless of coal prohibition in ARS and had a certain impact on air quality of BUA. In consequence, coal combustion was still a main contributor of atmospheric PAHs although the civil coal combustion was completely forbidden in BUA.

The shares of four types of emission sources fluctuated significantly during WSP due to the varied emission intensities and weather conditions. The VE and IN peaked on July 4 and June 29, which were 73.4% and 56.7%, respectively. BB possessed the largest number of peaks and they were 52.5% of June 21, 65.8% of June 23, 61.4% of June 27, and 80.7% of July 6. The time with occurrence of the BB peaks was almost same between ARS and BUA reflected the straw burning related PAHs had a certain impact on BUA.

Accompanied with the change of time, BB increased from 17.3% of DWH to 37.1% of AWH, being indicative of the impact of open burning of wheat straw in ARS on BUA. Certain contribution ratio of BB in DWH confirmed that biomass was still an important fuel in surrounding rural areas of Baoding driven by economic interests. CC accounted for the highest share of 37.9% in BUA during DWH implied that significant influence of CC in ARS on BUA. VE changed from 18.6% of DWH to 23% of AWH might be resulted from the increase of traffic flow due to the summer vacation.

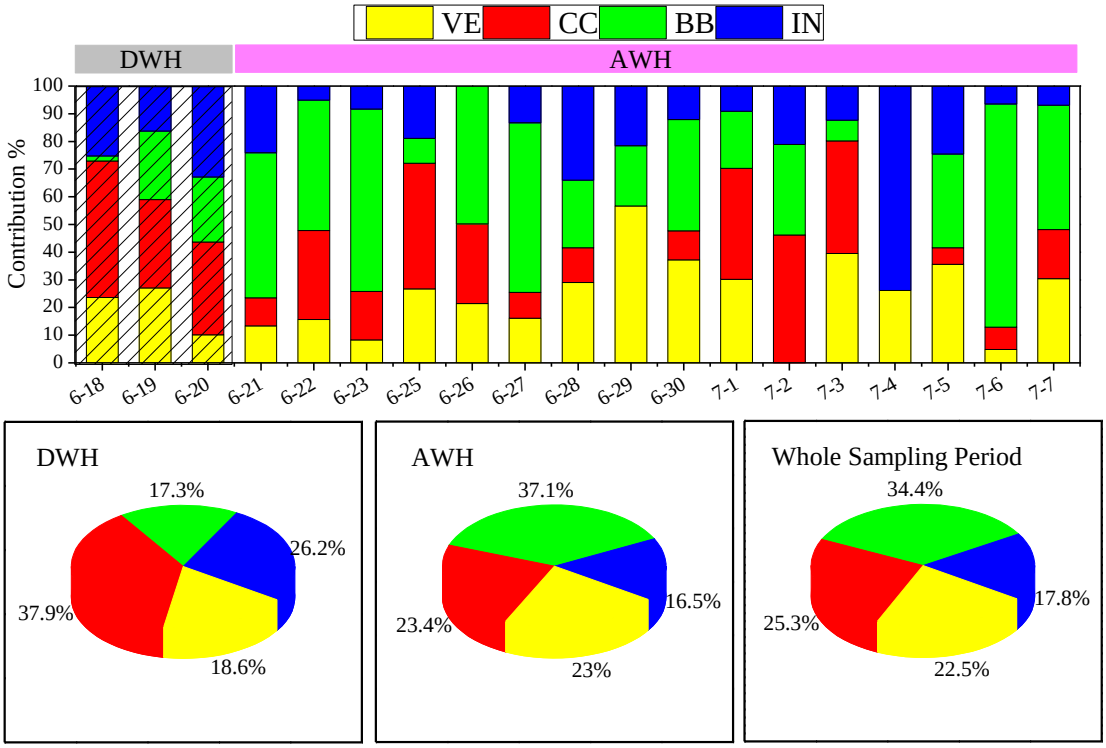

Fig. 5. Time series of contributions to PAHs by four sources and source contributions for DWH, AWH, and whole sampling period.

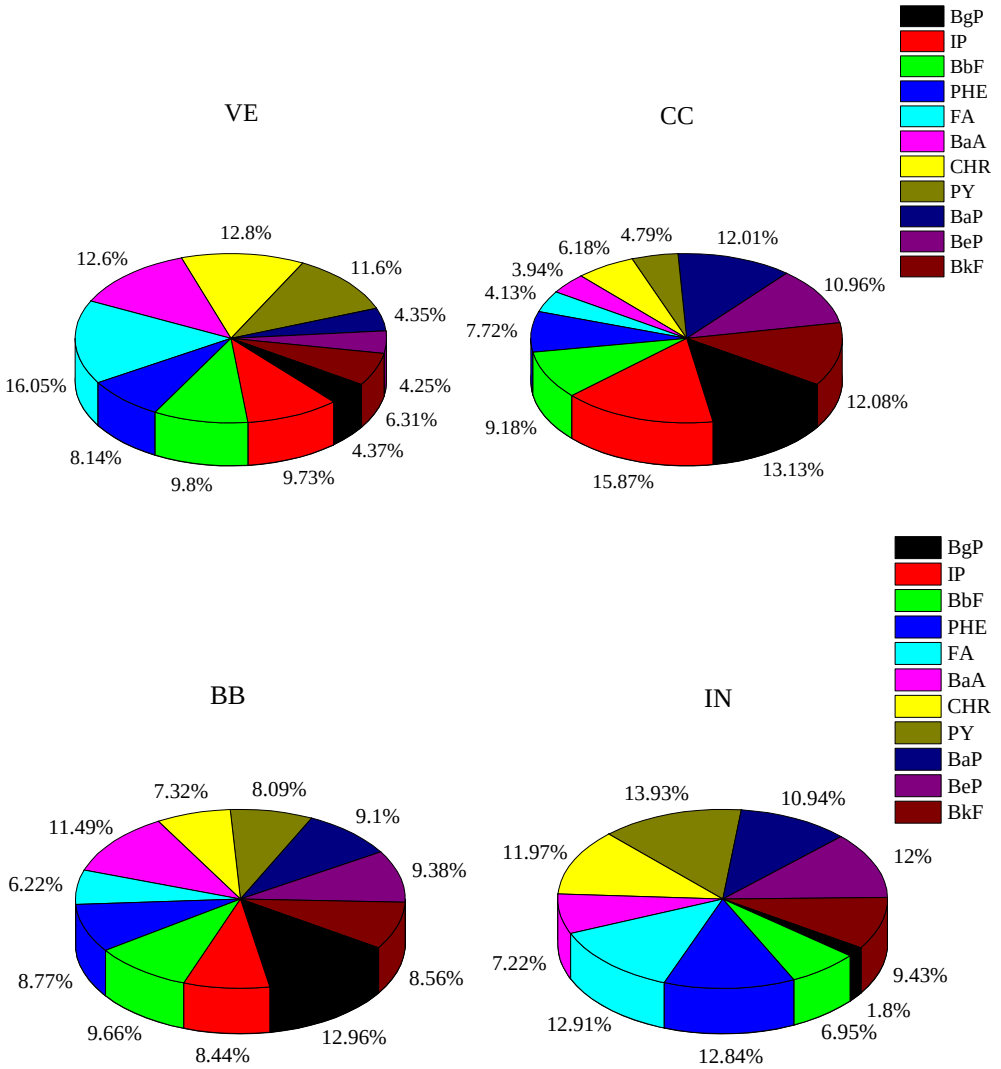

Fig. 6. Contributions of four sources to each PAH congener.

Fig. 6 presented the contributions of four sources for eleven individual PAH congeners. Similar to ARS in Wangdu County, the contributions of four source varied significantly among different PAH congeners. In regard to the PAH congeners with high levels, the main donors of were BB, IN, and CC for BeP, BB and CC for BgP, CC, BB, and VE for BbF, VE and IN for FA, CHR, and PY, CC, BB, and IN for BaP, respectively.

3.4 Backward Trajectory Clustering

Fig. S2 showed the backward trajectory curves during different periods including DWH, AWH, and WSP. There were four wind pathways for the three periods. In regard to DWH, 11.1% of air trajectories came from northern Mongolia, 30.0% from Cangzhou City and Bohai Bay, 33.3% from Fuping, Laiyuan County and east Shanxi province, 25.6% from southwest Shandong province, northern Henan Province, Handan, Xingtai and Shijiazhuang. It should be noted that the 33.3% of air masses originated from mountainous areas within Fuping County, Laiyuan County, Quyang County and Shanxi Province could bring large amounts of PAHs and $PM_{2.5}$ associated with indoor cooking fueled with biomass into BUA during DWH (Li *et al.*, 2020). The inputs of fugitive dust derived from the wheat straw stirring by harvesters in adjacent rural areas and desert of Mongolia resulted in high $PM_{2.5}$ levels of BUA during DWH.

The significant difference existed between BUA and ARS based on their air mass trajectories during AWH. 7.53% of the tracks came from northern Baoding, Beijing, Zhangjiakou and southern Mongolia, 43.55% from Bohai Bay, 40.86% from Shijiazhuang and Xingtai, and southern Baoding,

and 8.06% from Southwest Mongolia, Shanxi province and west Baoding City. 40.9% air masses arrived at BUA passed through Wangdu County furtherly proved the strong impact of biomass burning after wheat harvest on air PAHs of BUA. Industrial emissions from nearby Shijiazhuang and surrounding rural areas would be the important PAH sources.

4 CONCLUSIONS

Baoding, locates in the central part of BTH, is frequently nagged by the severe air pollution events in recent years. BTH is an important wheat producing base in China and its air quality can be deteriorated by $PM_{2.5}$ and PAHs associating with the activities of wheat harvest and subsequent straw burning for maize planting. Our previous study investigated the impact of wheat harvest associated behaviors on $PM_{2.5}$ and PAHs for ARS within Baoding city, which indicated the wheat harvest associated fugitive dust dramatically elevated the $PM_{2.5}$ levels in DWH and PAHs levels were also markedly promoted by straw burning in AWH.

In this study, $PM_{2.5}$ samples were systematically collected in BUA during DWH and AWH to investigate the levels of $PM_{2.5}$ and 18 PAHs, and PAH sources.

1) "Migration Effect" occurred during WSP, which caused the similar $PM_{2.5}$ fluctuation trends between ARS of Wangdu County and BUA. Compared with the ARS, the emergence of the peaks of $PM_{2.5}$ concentrations and PAH contents in BUA has a certain lag, and also the corresponding values in BUA were lower than those of ARS. Combination of the wind speed and direction during WSP with occurrence of pollutant peaks in BUA suggested that input effects of $PM_{2.5}$ in DWH and PAHs in AWH from rural areas.
2) Higher $PM_{2.5}$ of 137 μg m^{-3} was found in DWH, 2.58 times 53.1 μg m^{-3} of AWH, which was similar to ARS mainly due to the large amounts of fugitive dust during DWH. Unlike $PM_{2.5}$, the reverse fluctuation trend was found for PAHs and higher PAHs appeared during AWH due to the straw burning for maize planting. AWH possessed substantially higher PAH content (reported in μg g^{-1}) as 179 than 27.8 of DWH.
3) BB was the biggest contributor, followed by CC, VE and IN. BB share was significantly elevated from 17.3% of DWH to 37.1% of AWH, indicating the influence of straw burning regardless of the prohibition of straw burning issued by government. It was worth mentioning that high VE portion occurred in ARS instead of BUA due to the intensive running of wheat harvesters and Rotary cultivators. The contributions of IN and CC in BUA were slightly higher and lower than those of rural site. In a word, the wheat harvest associating activities promoted the assimilation of air quality in urban area into that of the ARS.
4) Backward trajectories clustering analysis showed that more than 40% air masses arrived at BUA passed through ARS of Wangdu County. The enterprises in surrounding rural areas and Shijiazhuang City would be the industrial source of PAHs in BUA.

ACKNOWLEDGEMENTS

This study was supported by the Natural Science Foundation of Hebei Province (B2020502007), the Beijing Natural Science Foundation (8212034), Foundation the Fundamental Research Funds for the Central Universities (2020MS125), the "Three Three Three Talent Project" of Hebei Province (A202001055), and Basic Research and Frontier Exploration Projects in Chongqing (the Natural Science Foundation of CQCSTC, cstc2018jcyjAX0776).

SUPPLEMENTARY MATERIAL

Supplementary data associated with this article can be found in the online version at https://doi.org/10.4209/aaqr.200625

REFERENCES

Bari, M.A., Kindzierski, W.B. (2016). Fine particulate matter ($PM_{2.5}$) in Edmonton, Canada: Source

apportionment and potential risk for human health. Environ. Pollut. 218, 219–229. https://doi.org/10.1016/j.envpol.2016.06.014

Cao, R., Zhang, H., Geng, N., Fu, Q., Teng, M., Zou, L., Gao, Y., Chen, J.P. (2018). Diurnal variations of atmospheric polycyclic aromatic hydrocarbons (PAHs) during three sequent winter haze episodes in Beijing, China. Sci. Total Environ. 625, 1486–1493. https://doi.org/10.1016/j.scitotenv.2017.12.335

Chen, P.F., Kang, S.C., Li, C.L., Li, Q.L., Yan, F.P., Guo, J.M., Ji, Z.M., Zhang, Q.G., Hu, Z.F., Tripathee, L., Sillanpää, M. (2018). Source apportionment and risk assessment of atmospheric polycyclic aromatic hydrocarbons in Lhasa, Tibet, China. Aerosol Air Qual. Res. 18, 1294–1304. https://doi.org/10.4209/aaqr.2017.12.0603

Chen, Y.C., Chiang, H.C., Hsu, C.Y., Yang, T.T., Lin, T.Y., Chen, M.J., Chen, N.T., Wu, Y.S. (2016). Ambient $PM_{2.5}$-bound polycyclic aromatic hydrocarbons (PAHs) in Changhua County, central Taiwan: Seasonal variation, source apportionment and cancer risk assessment. Environ. Pollut. 218, 372–382. https://doi.org/10.1016/j.envpol.2016.07.016

Cheng, Z., Wang, S., Fu, X., Watson, J.G., Jiang, J., Fu, Q., Chen, C., Xu, B., Yu, J., Chow, J.C., Hao, J. (2014). Impact of biomass burning on haze pollution in the Yangtze River delta, China: A case study in summer 2011. Atmos. Chem. Phys. 14, 4573–4585. https://doi.org/10.5194/acp-14-4573-2014

Dat, N.D., Lyu, J.M., Chang, M.B. (2018). Variation of atmospheric PAHs in Northern Taiwan during winter and summer seasons. Aerosol Air Qual. Res. 18, 1019–1031. https://doi.org/10.4209/aaqr.2018.01.0038

Ding, A.J., Huang, X., Nie, W., Chi, X.G., Xu, Z., Zheng, L.F., Xu, Z.N., Xie, Y.N., Qi, X.M., Shen, Y.C., Sun, P., Wang, J.P., Wang, L., Sun, J.N., Yang, X.Q., Qin, W., Zhang, X.Z., Cheng, W., Liu, W.J., Pan, L.B., Fu, C.B. (2019). Significant reduction of $PM_{2.5}$ in eastern China due to regional-scale emission control: Evidence from SORPES in 2011-2018. Atmos. Chem. Phys. 19, 11791–11801. https://doi.org/10.5194/acp-19-11791-2019

Elorduy, I., Elcoroaristizabal, S., Durana, N., García, J.A., Alonso, L. (2016). Diurnal variation of particle-bound PAHs in an urban area of Spain using TD-GC/MS: Influence of meteorological parameters and emission sources. Atmos. Environ. 138, 87–98. https://doi.org/10.1016/j.atmosenv.2016.05.012

Garcia-Suastegui, W.A., Huerta-Chagoya, A., Carrasco-Colin, K., Pratt, M.M., John, K., Petrosyan, P., Rubio, J., Poirier, M., Gonsebatt, M.E. (2011). Seasonal variations in the levels of PAH–DNA adducts in young adults living in Mexico City. Mutagenesis 26, 385–391. https://doi.org/10.1093/mutage/geq104

Han, S., Lee, J.Y., Heo, J., Kim, Y.P. (2019). Temporal trend of the major contributors for the particulate polycyclic aromatic hydrocarbons (PAHs) in Seoul. Aerosol Air Qual. Res. 19, 318–330. https://doi.org/10.4209/aaqr.2018.06.0231

Hays, M.D., Fine, P.M., Geron, C.D., Kleeman, M.J., Gullett, B.K. (2005). Open burning of agricultural biomass: Physical and chemical properties of particle-phase emissions. Atmos. Environ. 39, 6747–6764. https://doi.org/10.1016/j.atmosenv.2005.07.072

Keith, L.H., Telliard, W. (1979). A. Priority pollutants. I. A perspective view. Environ. Sci. Technol. 13, 416–423. https://doi.org/10.1021/es60152a601

Koss, A.R., Sekimoto, K., Gilman, J.B., Selimovie, V., Coggon, M.M., Zarzana, K.J., Yuan, B., Lerner, B.M., Brown, S.S., Jimenez, J.L., Krechmer, J., Roberts, J.M., Warneke, C., Yokelson, R.J., Gouw, J.D. (2018). Non-methane organic gas emissions from biomass burning: Identification, quantification, and emission factors from PTR–ToF during the FIREX 2016 laboratory experiment. Atmos. Chem. Phys. 18, 3299–3319. https://doi.org/10.5194/acp-18-3299-2018

Lelieveld, J., Evans, J.S., Fnais, M., Giannadaki, D., Pozzer, A. (2015). The contribution of outdoor air pollution sources to premature mortality on a global scale. Nature 525, 367–371. https://doi.org/10.1038/nature15371

Li, J.F., Song, Y., Mao, Y., Mao, Z.C., Wu, Y.S., Li, M.M., Huang, X., He, Q.C., Hu, M. (2014). Chemical characteristics and source apportionment of $PM_{2.5}$ during the harvest season in eastern China's agricultural regions. Atmos. Environ. 92, 442–448. https://doi.org/10.1016/j.atmosenv.2014.04.058

Li, M.N., Zhang, L.L. (2014). Haze in China: current and future challenges. Environ. Pollut. 189, 85–86. https://doi.org/10.1016/j.envpol.2014.02.024

Li, X.X., Kong, S.F., Yin, Y., Li, L., Yuan, L., Li, Q., Xiao, H., Chen, K. (2016). Polycyclic aromatic hydrocarbons (PAHs)in atmospheric $PM_{2.5}$ around 2013 Asian Youth Games period in Nanjing. Atmos. Res. 174, 85–96. https://doi.org/10.1016/j.atmosres.2016.01.010

Li, Z.Y., Fan, L., Wang, L., Ma, H.Q., Hu, Y., Jiang, Y.J., An, C.X., Liu, A.Q., Han, J.B., Jin, H. (2018). PAH Profiles of Emitted Ashes from Indoor Biomass Burning across the Beijing–Tianjin–Hebei Region and Implications on Source Identification. Aerosol Air Qual. Res. 18, 749–761. https://doi.org/10.4209/aaqr.2017.12.0588

Li, Z.Y., Wang, Y.T., Hu, Y., Chen, L., Zhu, H.T. (2019a). Emissions of NO_x, PM, SO_2, and VOCs from coal-fired boilers related to coal washing, iron-steel production, and lime and gypsum making in Shanxi, China. Aerosol Air Qual. Res. 19, 2056–2069. https://doi.org/10.4209/aaqr.2019.07.0363

Li, Z.Y., Wang, Y.T., Guo, S.T., Li, Z.X., Xing, Y.R., Liu, G.Q., Fang, R., Hu, Y., Zhu, H.T., Yan, Y.L. (2019b). $PM_{2.5}$ associated PAHs and inorganic elements from combustion of biomass, cable wrapping, domestic waste, and garbage for power generation. Aerosol Air Qual. Res. 19, 2502–2517. https://doi.org/10.4209/aaqr.2019.10.0495

Li, Z.Y., Guo, S.T., Li, Z.X., Wang, Y.T., Hu, Y., Xing, Y.R., Liu, G.Q., Fang, R., Zhu, H.T. (2020a). $PM_{2.5}$ associated phenols, phthalates, and water soluble ions from five stationary combustion sources. Aerosol Air Qual. Res. 20, 61–71. https://doi.org/10.4209/aaqr.2019.11.0602

Li, Z.Y., Wang, Y.T., Li, Z.X., Guo, S.T., Hu, Y. (2020b). Levels and sources of $PM_{2.5}$–associated PAHs during and after the wheat harvest in a central rural area of the Beijing–Tianjin–Hebei (BTH) region. Aerosol Air Qual. Res. 20, 1070–1082. https://doi.org/10.4209/aaqr.2020.03.0083

Liu, Y., Yan, C.Q., Ding, X., Wang, X.M., Fu, Q.Y., Zhao, Q.B., Zhang, Y.H, Duan, Y.H, Qiu, X.H., Zheng, M. (2017). Sources and spatial distribution of particulate polycyclic aromatic hydrocarbons in Shanghai, China. Sci. Total Environ. 584–585, 307–317. https://doi.org/10.1016/j.scitotenv.2016.12.134

Manoli, E., Samara, C. (1999). Polycyclic aromatic hydrocarbons in natural waters: Sources, occurrence and analysis. Trac. Trends Anal. Chem. 18, 417–428. https://doi.org/10.1016/S0165-9936(99)00111-9

Martellini, T., Giannoni, M., Lepri, L., Katsoyiannis, A., Cincinelli, A. (2012). One year intensive $PM_{2.5}$ bound polycyclic aromatic hydrocarbons monitoring in the area of Tuscany, Italy. Concentrations, source understanding and implications. Environ. Pollut. 164, 252–258. https://doi.org/10.1016/j.envpol.2011.12.040

Ravindra, K., Bencs, L., Wauters, E., de Hoog, J., Deutsch, F., Roekens, E., Bleux, N., Berghmans, P., Van Grieken, R. (2006). Seasonal and site–specific variation in vapour and aerosol phase PAHs over Flanders (Belgium) and their relation with anthropogenic activities. Atmos. Environ. 40, 771–785. https://doi.org/10.1016/j.atmosenv.2005.10.011

Ravindra, K., Singh, T., Mor, S. (2019). Emissions of air pollutants from primary crop residue burning in India and their mitigation strategies for cleaner emissions. J. Clean. Prod. 208, 261–273. https://doi.org/10.1016/j.jclepro.2018.10.031

Sarigiannis, D.A., Karakitsios, S.P., Zikopoulos, D., Nikolaki, S., Kermenidou, M. (2015). Lung cancer risk from PAHs emitted from biomass combustion. Environ. Res. 137, 147–156. https://doi.org/10.1016/j.envres.2014.12.009

Shen, H.Z., Huang, Y., Wang, R., Zhu, D., Li, W., Shen, G.F., Wang, B., Zhang, Y.Y., Chen, Y.C., Lu, Y., Chen, H., Li, T.C., Sun, K., Li, B.G., Liu, W.X., Liu, J.F., Tao, S. (2013). Global atmospheric emissions of polycyclic aromatic hydrocarbons from 1960 to 2008 and future predictions. Environ. Sci. Technol. 47, 6415–6424. https://doi.org/10.1021/es400857z

Simayi, M., Yahefu, P., Han, M.X. (2018). Spatiotemporal variation, source analysis, and health risk assessment of particle–bound PAHs in Urumqi, China. Aerosol Air Qual. Res. 18, 2728–2740. https://doi.org/10.4209/aaqr.2018.04.0151

Tan, J.H., Zhang, L.M., Zhou, X.M., Duan, J.C., Li, Y., Hu, J.H., He, K.B. (2017). Chemical characteristics and source apportionment of $PM_{2.5}$ in Lanzhou, China. Sci. Total Environ. 601, 1743–1752. https://doi.org/10.1016/j.scitotenv.2017.06.050

Wang, X.Q., Wei, W., Cheng, S.Y., Li, J.B., Zhang, H.Y., L, Z. (2018). Characteristics and classification of $PM_{2.5}$ pollution episodes in Beijing from 2013 to 2015. Sci. Total Environ. 612, 170–179. https://doi.org/10.1016/j.scitotenv.2017.08.206

Wu, D., Wang, Z.S., Chen, J.H., Kong, S.F., Fu, X., Deng, H.B., Shao, G.F., Wu, G. (2014). Polycyclic

aromatic hydrocarbons (PAHs) in atmospheric $PM_{2.5}$ and PM_{10} at a coal-based industrial city: Implication for PAH control at industrial agglomeration regions, China. Atmos. Res. 149, 217–229. https://doi.org/10.1016/j.atmosres.2014.06.012

Wu, Y., Yang, L., Zheng, X., Zhang, S.J., Song, S.J., Li, J.Q., Hao, J.M. (2014). Characterization and source apportionment of particulate PAHs in the roadside environment in Beijing. Sci. Total Environ. 470–471, 76–83. https://doi.org/10.1016/j.scitotenv.2013.09.066

Xing, X.L., Zhang, Y., Yang, D., Zhang, J.Q., Chen, W., Wu, C.X., L, H.X., Q, S.H. (2016). Spatio-temporal variations and influencing factors of polycyclic aromatic hydrocarbons in atmospheric bulk deposition along a plain-mountain transect in western China. Atmos. Environ. 139, 131–138. https://doi.org/10.1016/j.atmosenv.2016.05.027

Xiong, Q.L., Zhao, W.J., Gong, Z.N., Zhao, W.H., Tang, T. (2015). Fine particulate matter pollution and hospital admissions for respiratory diseases in Beijing, China. Int. J. Environ. Res. Public Health 12, 11880–11892. https://doi.org/10.3390/ijerph120911880

Yao, L., Yang, L.X., Yuan, Q., Yan, C., Dong, C., Meng, C.P., Sui, X., Yang, F., Lu, Y.L., Wang, W.X. (2016). Sources apportionment of $PM_{2.5}$ in a background site in the North China Plain. Sci. Total. Environ. 541, 590–598. https://doi.org/10.1016/j.scitotenv.2015.09.123

Zhai, S.X., Jacob, D.J., Wang, X., Shen, L., Li, K., Zhang, Y.Z., Gui, K., Zhao, T.L., Liao, H. (2019). Fine particulate matter ($PM_{2.5}$) trends in China, 2013-2018: contributions from meteorology. Atmos. Chem. Phys. 19, 11031–11041. https://doi.org/10.5194/acp-2019-279

Zhang, X.H., Lu, Y., Wang, Q.G., Qian, X. (2019a). A high–resolution inventory of air pollutant emissions from crop residue burning in China. Atmos. Environ. 213, 207–214. https://doi.org/10.5194/acp-2017-1113

Zhang, Y., Tao, S. (2009). Global atmospheric emission inventory of polycyclic aromatic hydrocarbons (PAHs) for 2004. Atmos. Environ. 43, 812–819. https://doi.org/10.1016/j.atmosenv.2008.10.050

Zhang, Y., Yang, L.X., Gao, Y., Chen, J.M., Li, Y.Y., Jiang, P., Zhang, J.M., Yu, H., Wang, W.X. (2019b). Comparative study of PAHs in PM_1 and $PM_{2.5}$ at a background site in the North China Plain. Aerosol Air Qual. Res. 19, 2281–2293. https://doi.org/10.4209/aaqr.2018.12.0462

Zhang, Z.Z., Wang, W.X., Cheng, M.M., Liu, S.J., Xu, J., He, Y.J., Meng, F. (2017). The contribution of residential coal combustion to $PM_{2.5}$ pollution over China's Beijing–Tianjin–Hebei region in winter. Atmos. Environ. 159, 147–161. https://doi.org/ 10.1016/j.atmosenv.2017.03.054

Zhou, J.B., Wang, T.G., Huang, Y.B., Mao, T., Zhong, N.N. (2005). Seasonal variation and spatial distribution of polycyclic aromatic hydrocarbons in atmospheric PM_{10} of Beijing, People's Republic of China. Bull. Environ. Contam. Toxicol. 74, 660–666. https://doi.org/10.1007/s00128-005-0634-y

Zhou, M., Wang, H., Zhu, J., Chen, W., Wang, L., Liu, S., Li, Y., Wang, L., Liu, Y., Yin, P., Liu, J., Yu, S., Tan, F., Barber, RM., Coates, M.M., Dicker, D., Fraser, M., González-Medina, D., Hamavid, H., … Liang, X. (2016). Cause-specific mortality for 240 causes in China during 1990–2013: A systematic subnational analysis for the Global Burden of Disease Study 2013. Lancet 387, 251–272. https://doi.org/10.1016/S0140-6736(15)00551-6